

Cell Reports Medicine, Volume 4

Supplemental information

Single-cell RNA sequencing reveals distinct

T cell populations in immune-related

adverse events of checkpoint inhibitors

Shoiab Bukhari, Brian S. Henick, Robert J. Winchester, Shalom Lerrer, Kieran Adam, Yevgeniya Gartshteyn, Rohan Maniar, Ziyang Lin, Alireza Khodadadi-Jamayran, Aristotelis Tsigos, Mary M. Salvatore, Galina G. Lagos, Steven L. Reiner, Matthew C. Dallos, Matthen Mathew, Naiyer A. Rizvi, and Adam Mor

A

| Patient Key | Clinical | Age | Gender | Tumor | Stage | irAE type | irAE grade | Steroids | Weeks to onset |
|-------------|-------------|-----|--------|----------|-------|---------------------------|------------|-----------------|----------------|
| P1 | Arthritis | 49 | Female | NSCLC | 4 | Musculoskeletal | 3 | Systemic | 4-6 |
| P2 | Arthritis | 62 | Female | NSCLC | 4 | Musculoskeletal | 2 | Systemic | 4-6 |
| P3 | Arthritis | 53 | Female | NSCLC | 3 | Musculoskeletal | 2 | Intra-articular | 4-6 |
| P4 | Thyroiditis | 73 | Male | NSCLC | 4 | Endocrine | 3 | None | N/A |
| P5 | Thyroiditis | 70 | Male | NSCLC | 4 | Endocrine | 3 | None | N/A |
| P6 | Thyroiditis | 76 | Male | NSCLC | 4 | Endocrine-Renal | 2 | Systemic | N/A |
| P7 | Arthritis | 65 | Female | NSCLC | 4 | Musculoskeletal | 2 | Systemic | 4-6 |
| P8 | Pneumonitis | 75 | Male | NSCLC | 4 | Pulmonary | 2 | Systemic | 4-6 |
| P9 | no irAE | 75 | Female | NSCLC | 4 | none | 0 | | No irAE |
| P10 | Pneumonitis | 51 | Female | NSCLC | 4 | Pulmonary | 3 | Systemic | 4-6 |
| P11 | Pneumonitis | 55 | Male | NSCLC | 4 | Pulmonary | 2 | Systemic | 4-6 |
| P12 | Pneumonitis | 72 | Male | NSCLC | 4 | Pulmonary | 2 | Systemic | 4-6 |
| P13 | Pneumonitis | 58 | Male | Prostate | N/A | Pulmonary | 3 | Systemic | 4-6 |
| P14 | Pneumonitis | 74 | Male | Prostate | N/A | Pulmonary | 3 | Systemic | 4-6 |
| P15 | Pneumonitis | 52 | Female | NSCLC | 4 | Pulmonary-Endocrine-Renal | 3 | Systemic | 4-6 |
| P16 | Neuritis | 65 | Female | NSCLC | 4 | Neuro-Gastrointestinal | 3 | Systemic | |
| P17 | no irAE | 67 | Male | NSCLC | 4 | none | 0 | None | No irAE |
| P18 | no irAE | 40 | Female | HNSCC | 4 | none | 0 | None | No irAE |
| P19 | no irAE | 74 | Male | HNSCC | 4 | none | 0 | None | No irAE |
| P20 | no irAE | 77 | Male | NSCLC | 4 | none | 0 | None | No irAE |
| P21 | no irAE | 81 | Male | NSCLC | 4 | none | 0 | None | No irAE |
| P22 | no irAE | 68 | Female | NSCLC | 4 | none | 0 | None | No irAE |
| P23 | no irAE | 69 | Male | Prostate | N/A | none | 0 | None | No irAE |
| P24 | no irAE | 66 | Male | Prostate | N/A | none | 0 | None | No irAE |

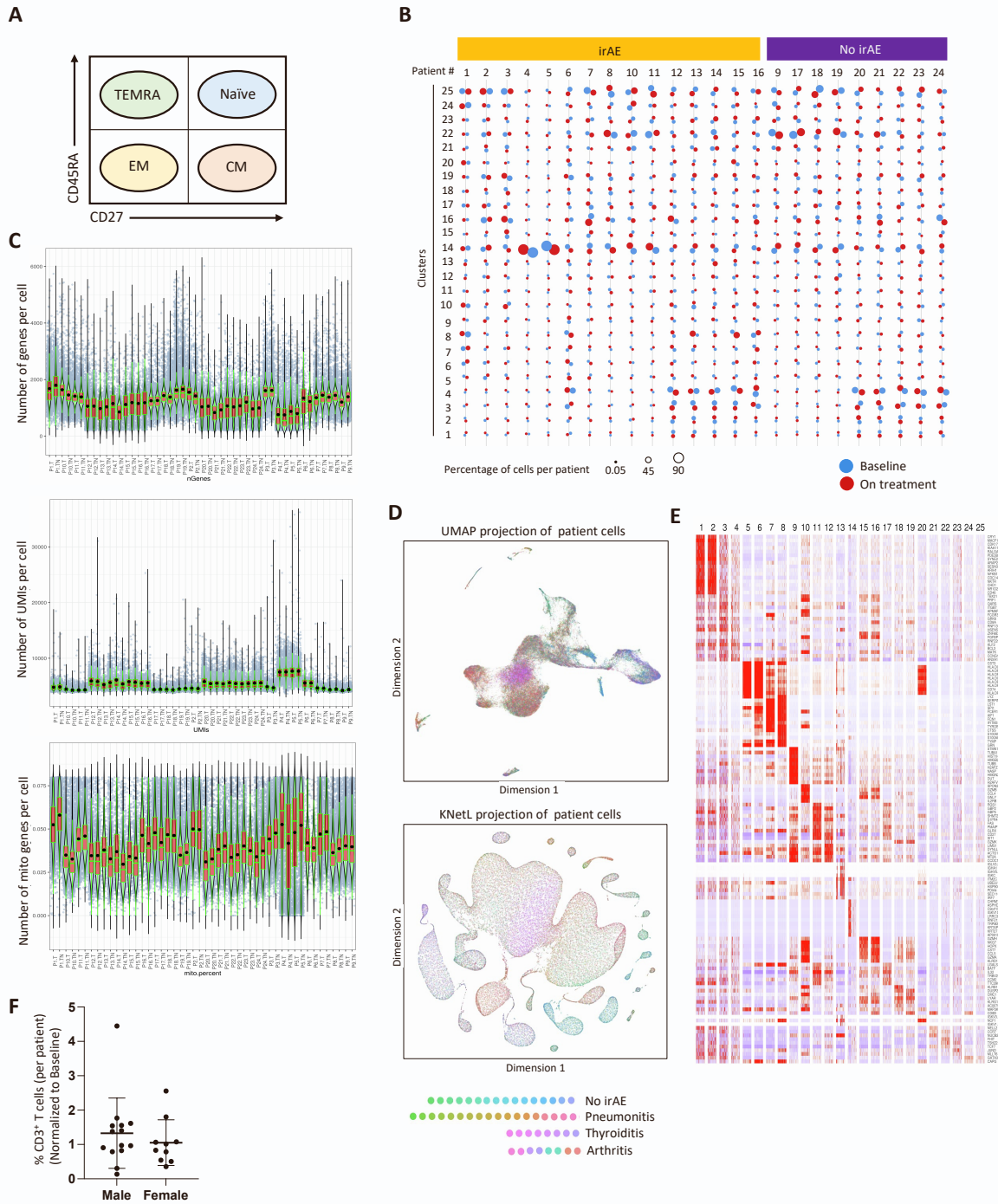
B

| Patients | | irAEs group |
|--------------------------|---------------|-------------|
| Age (average) | | 70 years |
| Gender (n) | Male | 62 |
| | Female | 73 |
| Tumor type | Lung | 46 |
| | GU | 37 |
| | Melanoma | 25 |
| | Other | 27 |
| Agent (ICIs) | Pembrolizumab | 28 |
| | Nivolumab | 41 |
| | Atezolizumab | 21 |
| | Durvalumab | 2 |
| | Combination | 43 |
| irAEs type | Joints | 58 |
| | Skin | 16 |
| | Neurologic | 16 |
| | Endocrine | 20 |
| | Pulmonary | 14 |
| | Other | 26 |
| irAEs grade | | 2.7 |
| Time to onset | | 57 days |
| Total number of patients | | 135 |

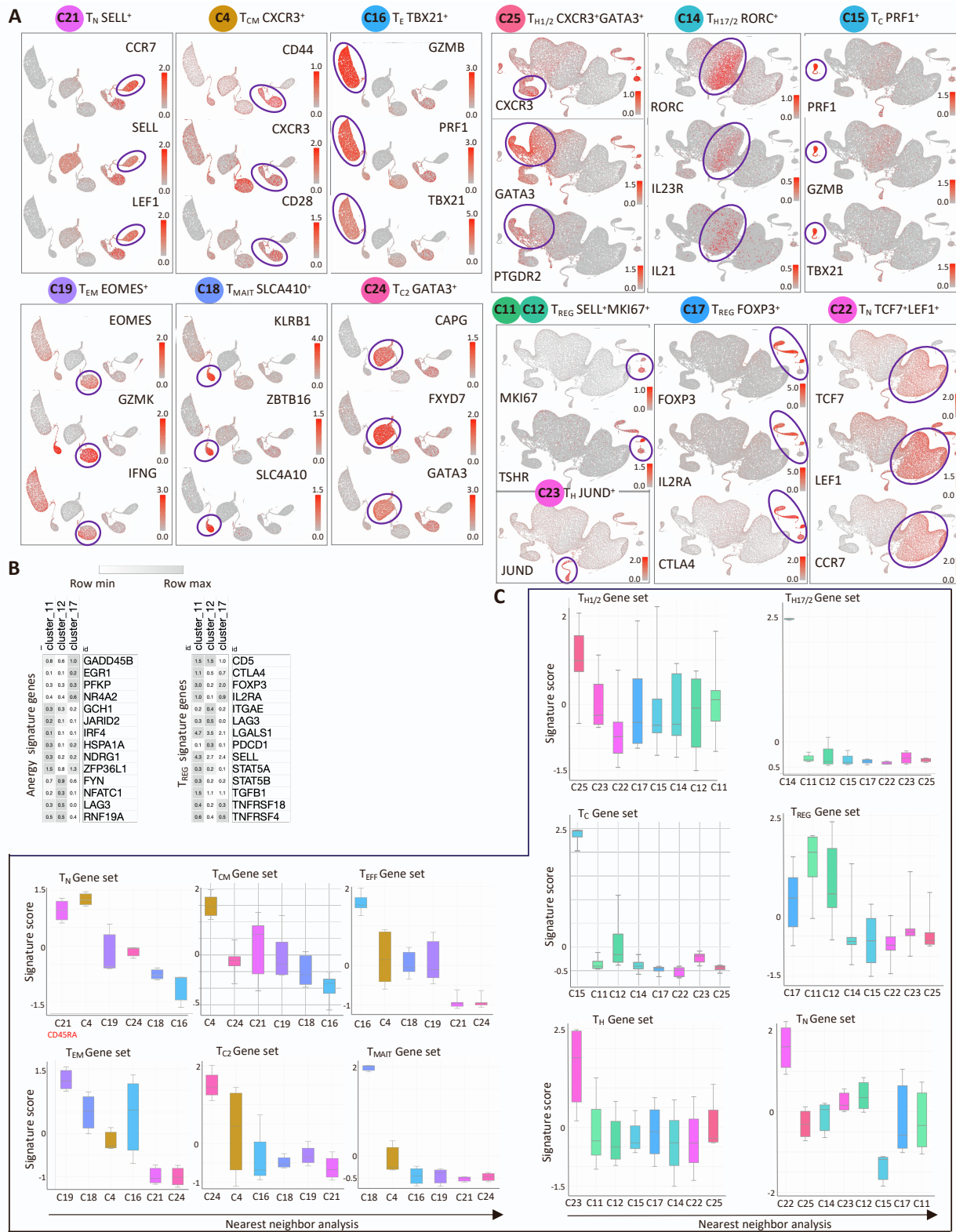
Table S1. Clinical characterization of the patients enrolled to the study, related to figure 1.

| CD8+ T cells annotation | | | | CD4+ T cells annotation | | | |
|-------------------------|-----------------|-------------------------------------|-------------|-------------------------|-----------------|-------------------------------------|-----------|
| Subset | Surface Markers | Intracellular/Transcription factors | Cytokines | Subset | Surface Markers | Intracellular/Transcription factors | Cytokines |
| Naïve | SELL | | | TH1 | KLRD1 | STAT1 | TNF |
| | IL7R | | | | IFNGR1 | STAT4 | LTA |
| | CCR7 | | | | CXCR3 | TBX21 | IFNG |
| | CD45RA | | | | CXCR6 | | IL2 |
| | CD27 | | | | CCR1 | | |
| | | | | | CCR5 | | |
| Effector | IL2RA | TBX21 | IFNG | | IL12RB1 | | |
| | TNFRSF8 | | IL2 | | IL18R1 | | |
| | CD69 | | PRF1 | | TNFSF11 | | |
| | TNFRSF4 | | GZMB / GZMA | | HAVCR2 | | |
| | ICOS | | TNFA | | | | |
| | KLRG1 | | CCL3 | | | | |
| | HAVCR2 | | CCL4 | TH2 | CXCR4 | BATF | IL4 |
| | | | CCL5 | | CCR4 | GATA3 | IL5 |
| | | | | | CCR8 | IRF4 | IL13 |
| | | | | | PTGDR2 | STAT6 | AREG |
| | | | | | HAVCR1 | | |
| Effector Memory | CD44 | EOMES | GZMK | | IL17RB | | |
| | CD45RO | | | | | | |
| | /CD45RA- | TBET | IFNG++ | | IL33 | | |
| | CD62L low | | TNFA++ | | | | |
| | CD127 high | | PRF1 | | | | |
| | KLRG1 high | | IL2 | | | | |
| | CCR7 low | | | TH17 | IL1R1 | AHR | CSF2 |
| | | | | | KLRB1 | BATF | IL17A |
| | | | | | CCR4 | MAF | IL17AF |
| Central Memory | CD45RO/CD45RA- | TBET | IFNG | | CCR6 | NFKBIZ | IL17F |
| | CD62L low | EOMES | IL2 | | IL21R | IRF4 | IL21 |
| | CD127 ++ | | TNFA | | IL12RB1 | RORA | IL22 |
| | CCR7 low | | | | | RORC | |
| | CD27 | | | | | STAT3 | |
| | CD28 | | | | | | |
| | CXCR3 mid | | | CD4 Cytotoxic | TBX21 | PRF1 | GZMB |
| | | | | | | | GZMA |
| MAIT cells | KLRB1 | SLC4A1 | | | | | |
| | | ZBTB16 | | | | | |
| | | | | TREG | CTLA4 | FOXP3 | |
| Regulatory | CD57 | B3GAT1 | | | IL2RA | | |
| | CD28- | | FOXP3 | | | | |
| | KLRG1++ | | IKAROS | | | | |
| | PD1 | | EGR1 | TFH | CXCR3 | BATF | IL21 |
| | LAG3 | | EGR2 | | CXCR5 | BCL6 | |
| | HLADR | | | | ICOS | MAF | |
| | | | | | PDCD1 | IFR4 | |
| | | | | | | STAT3 | |
| TRMs | CD69+ | | ITGA1 | | | | |
| | CD103+/- | | ITGAE | | | | |
| | CD101 | | SELPLG | | | | |
| | CD49a | | Hobit | | | | |
| | PD1 | | Blimp1 | | | | |
| | CXCR6 | | Runx3 | | | | |
| | CLA | | Notch/RBPJ | | | | |
| | CCR8 | | | | | | |

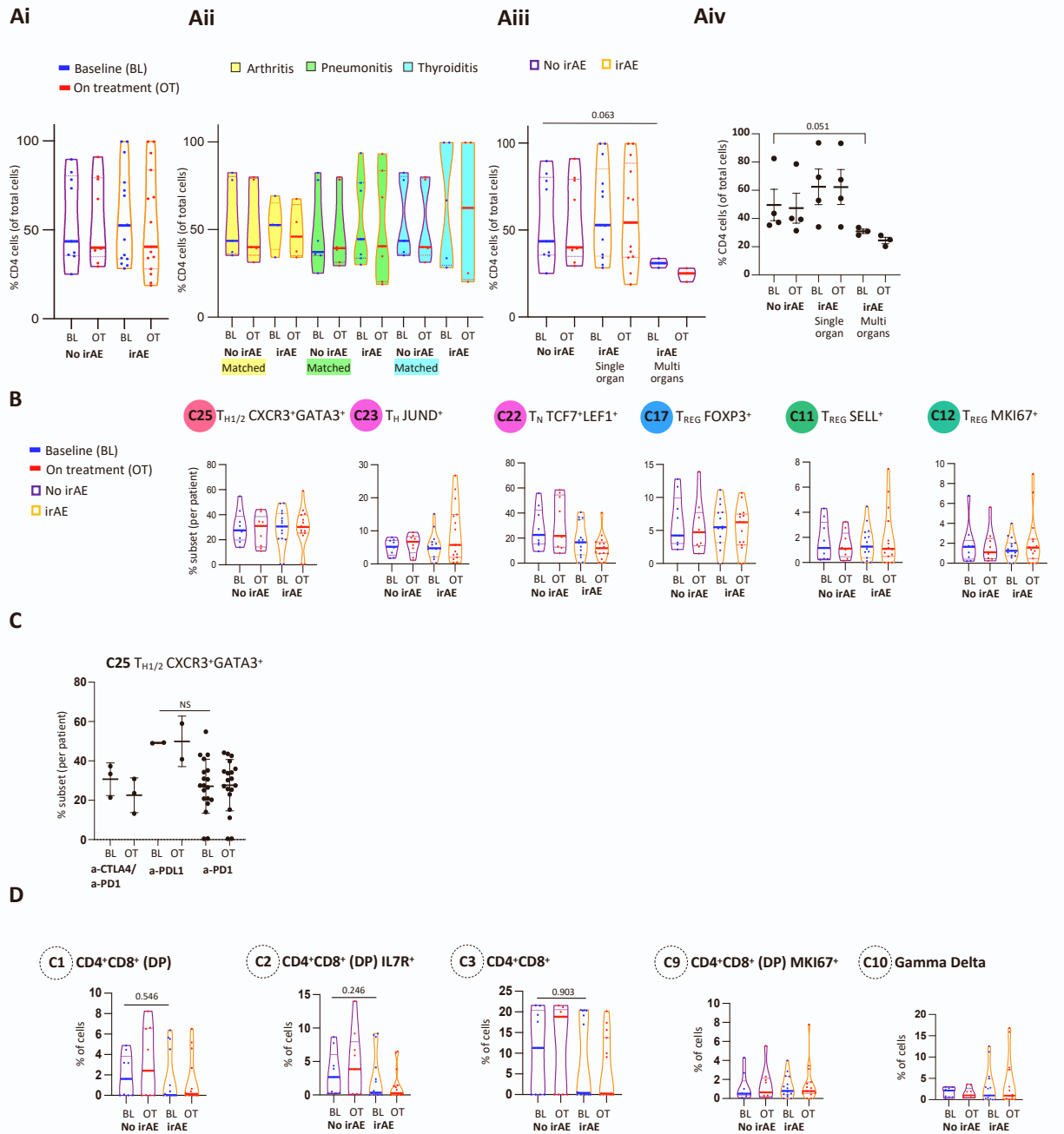
Table S2. T cell subset markers, related to figure 2.



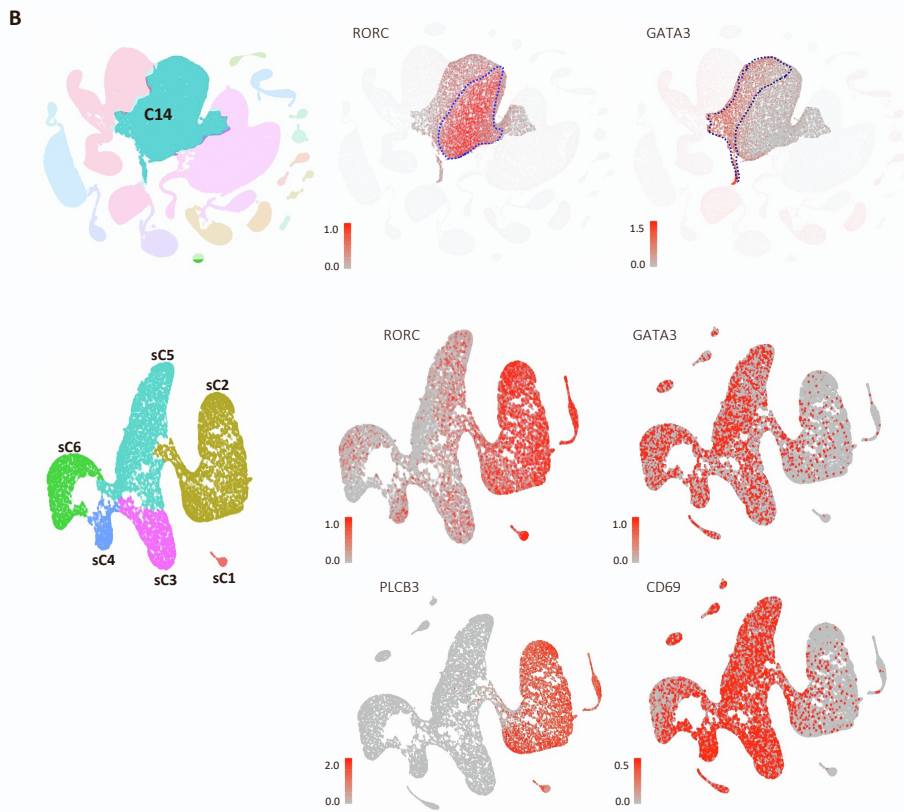
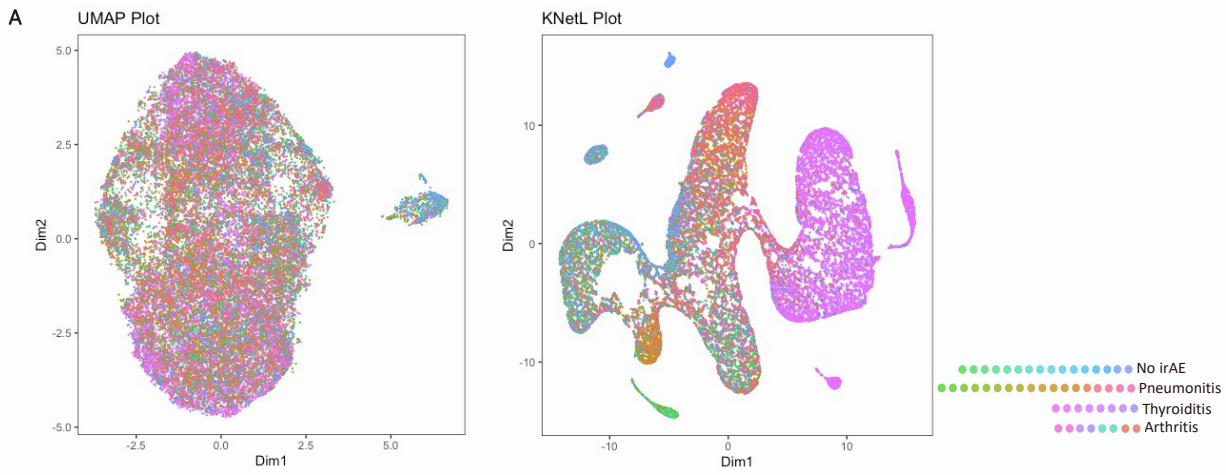
Supplemental figure 1. T cells annotation and characterization, related to figure 2. (A) T cells were annotated into Naïve, central memory (CM), effector memory (EM), terminally differentiated (TEMRA) maturation subsets based on expression levels of CD27 and CD45RA. (B) Qualitative representation of T cell abundances at baseline and on treatment within each cluster per patient using Beeswarm map. (C) Quality control bar plots showing the number of genes, UMI, mito genes per cell. (D) UMAP and KNetL projection of cells contributed by each patient. (E) Heatmap representation of cluster defining marker genes and other cluster associated genes. (F) Dot plot representing the total T cell distribution in males compared to females. Statistical significance: T test, unpaired Mann-Whitney, P-value, Exact-two-tailed, the center lines denote the mean of SEM. T (on treatment) TN (baseline).



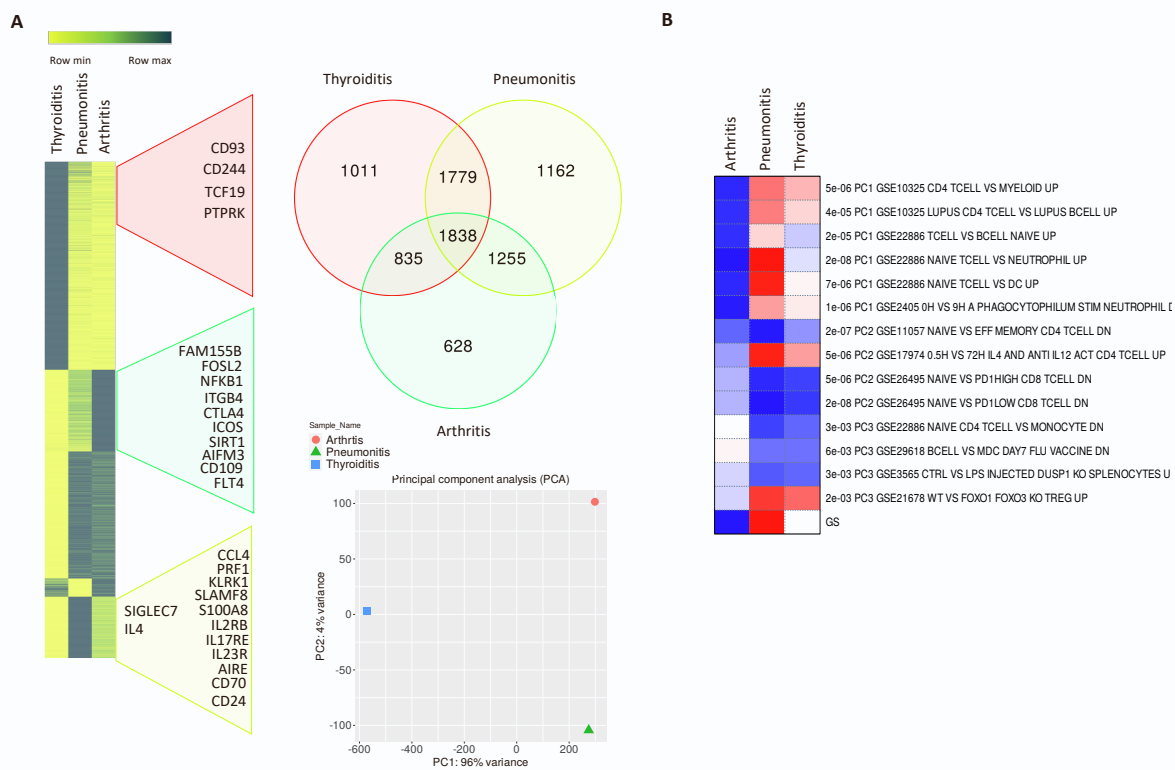
Supplemental figure 2. Gene markers of T cell subsets, related to figure 2. (A) KNetL plots projecting the RNA expression of marker genes indicated in red. Each red dot represents a cell. (B) Heatmap representation of RNA expression of anergy and T_{REG} marker genes sets. (C) Bar graphs indicating the marker gene sets score for each subset cluster, further resolved in the basis of nearest between the marker gene sets.



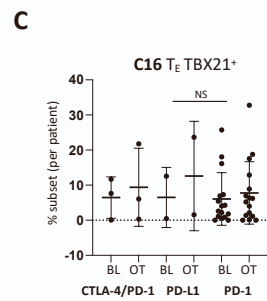
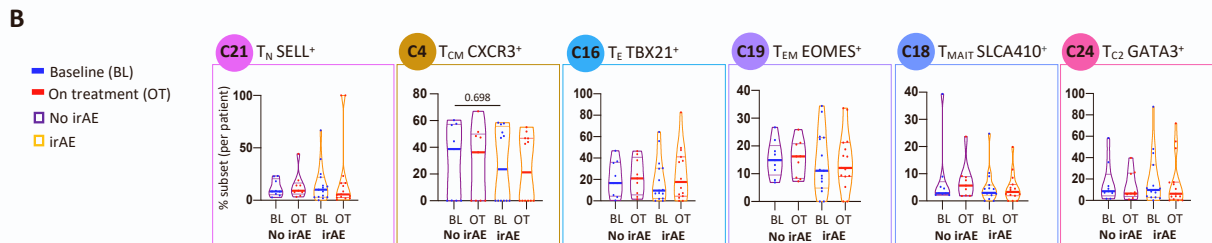
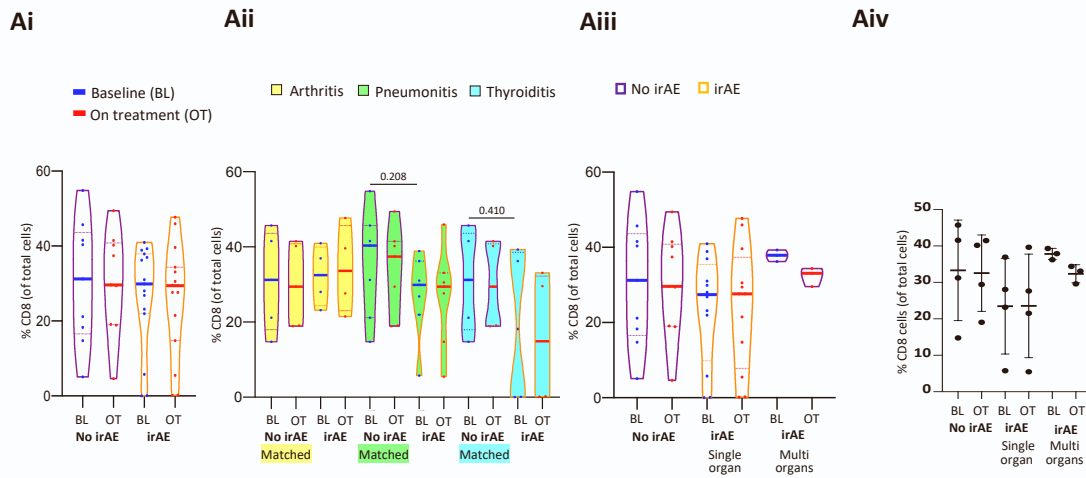
Supplemental figure 3. Characterization of CD4 T cells, related to figure 3. Percentages distribution of subset of CD4 T cells between no irAE and the different irAE groups of patients at baseline and on treatment (A). Percentages of CD4 specific clusters among patients with and without irAEs and baseline and on treatment with ICIs (B). Percentages of cells of cluster 25 based on the specific type of ICIs used (C). Double positive and gamma delta T cells (D).



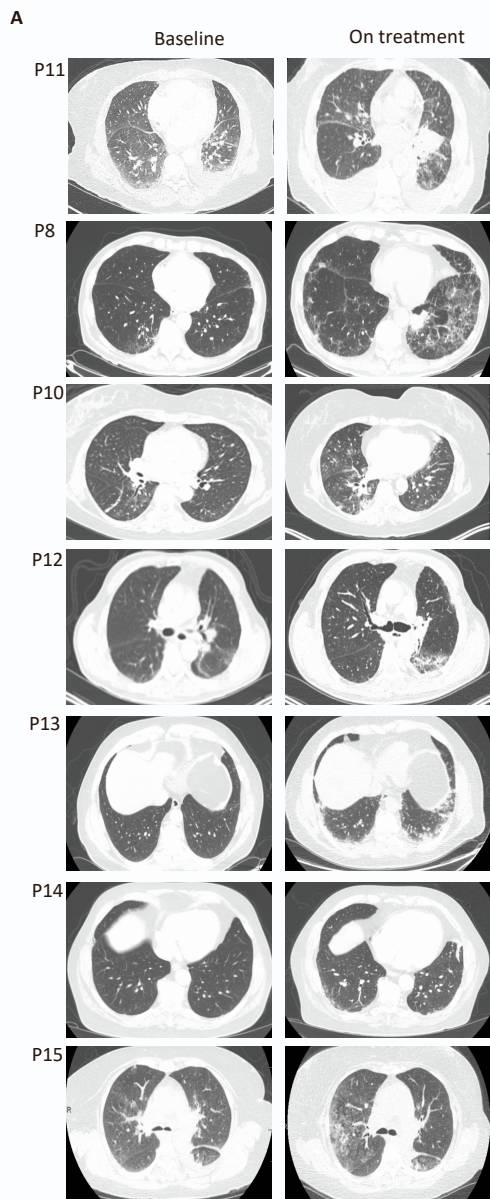
Supplemental figure 4. Characterization of the T cells in cluster 14, related to figure 4. (A) UMAP and KNetL projections of cells from sub-clustering of meta-cluster 14. (B) KNetL projection of marker gene RORC, GATA3, PLCB3, and CD69.



Supplemental figure 5. Organ specific toxicities and association with gene expression, related to figure 4. Heat map, Venn diagram, and PCA plot of the different genes that characterize patient with arthritis, thyroiditis and pneumonitis irAEs (A). Comparison of organ specific irAEs genes and published GSE studies (B).



Supplemental figure 6. Characterization of CD8 T cells, related to figure 5. Percentages of CD8 cell clusters among patients with different types of irAEs (A). Percentages of specific clusters of cells of patients with and without irAEs. Percentages of subset of patients treated with different types of ICIs (C).



B

| Patient No. | Pneumonitis Pattern | Tumor type | irAE grade | Size Dominant nodule (mm) | Location of nodule |
|-------------|---------------------|------------|------------|---------------------------|--------------------|
| P8 | CHP | NSCLC | 2 | 26 | LUL |
| P10 | CHP | NSCLC | 3 | 77 | RLL |
| P11 | CHP | NSCLC | 2 | 37 | RLL |
| P12 | OP | NSCLC | 2 | 18 | LLL |
| P13 | OP | Prostate | 3 | 0 | NA |
| P14 | OP | Prostate | 3 | 0 | NA |
| P15 | OP | NSCLC | 3 | 67 | LLL |

Supplemental figure 7. CT scans of pneumonitis patients at baseline and on treatment, related to figure 6. CT scan images (A). Clinical characterization of irAE patients that developed pneumonitis (B).